Mechanical properties and strength evolution model of sandstone considering the coupling impact of freeze and thaw weathering process and confining pressure

Xin Xiong (xiongxin@csu.edu.cn)
Central South University
Keping Zhou
Central South University
Feng Gao
Central South University
Chun Yang
Central South University
Jielin Li
Central South University

Research Article

Keywords: Freeze and thaw weathering cycles, confining pressure, confining pressure increase factor (CPIF), strength evolution model, nuclear magnetic resonance (NMR)

Posted Date: March 11th, 2022

DOI: https://doi.org/10.21203/rs.3.rs-1436924/v1

Mechanical properties and strength evolution model of sandstone considering the coupling impact of freeze and thaw weathering process and confining pressure

Xin Xiong[a, b], Keping Zhou[a, b], Feng Gao[a, b, *], Chun Yang[a, b, *], Jielin Li[a, b]

[a] *School of Resource and Safety Engineering, Central South University, Changsha, Hunan 410083, PR China*

[b] *Research Center for Mining Engineering and Technology in Cold Regions, Central South University, Changsha, Hunan 410083, PR China*

* Corresponding author at: School of Resource and Safety Engineering, Central South University, Changsha, Hunan 410083, PR China

E-mail address: csugaofeng@csu.edu.cn (Feng Gao); chunyang@csu.edu.cn (Chun Yang)

Abstract

Freeze and thaw (F&T) weathering cycles induced by day-night and seasonal temperature changes cause a large number of rock mass engineering disasters in cold areas. Investigating the impact of F&T weathering process on strength and deformation characteristics of frozen-thawed rocks is therefore of critical scientific importance for evaluating the stability and optimizing the design of rock mass engineering in these areas. In this research, the evolution characteristics of F&T damage were analysed based on T_2 spectrum distribution curves of sandstone specimens before and after F&T weathering cycles. The coupling impact of the quantity of F&T weathering cycles and confining pressure on pre-peak and post-peak deformation behaviours of sandstone specimens were analysed in detail. By introducing the confining pressure increase factor (CPIF), the impact of confining pressure on triaxial compressive strength (TCS) of sandstone specimens after undergoing different quantities of F&T weathering cycles was further investigated. A novel strength evolution model was proposed that could effectively describe the coupling impact of the quantity of F&T weathering cycles and confining pressure on TCS of rocks after undergoing F&T weathering process. The proposed strength evolution model was cross-verified with experimental data from the published literature, and all correlation coefficients are above 0.95, which proves that the strength evolution model proposed in this paper is reasonable; in addition, this model has strong applicability.

Keywords

Freeze and thaw weathering cycles; confining pressure; confining pressure increase factor (CPIF); strength evolution model; nuclear magnetic resonance (NMR).

1 Introduction

During the construction of rock mass engineering (such as mines, roads and tunnels) in cold regions, the recurrence of F&T weathering processes induced by day-night and seasonal temperature changes causes rapid damage and the deterioration of rock masses and has initiated a large number of F&T disasters, such as rock falls, landslides(Matsuoka 2001; Matsuoka 2008; Nicholson and Nicholson 2000) and the cracking of rock surrounding tunnels(Lai et al. 2000; Zhang et al. 2004), which has a major impact on the design, construction and operation of rock mass engineering in cold areas. The strength and deformation behaviours of rocks are the theoretical basis for evaluating the stability and optimizing the engineering design of rock mass engineering(Kang et al. 2017). Therefore, investigating mechanical properties of rocks after undergoing F&T weathering cycles has great significance in evaluating the stability and optimizing the design of rock mass engineering in cold areas.

The impact of F&T weathering process on rock mechanical properties have been investigated by a considerable number of scholars. These investigation results indicate that after rocks (such as sandstone, tuff, gneiss, granite and shale) being underwent F&T weathering process, elastic modulus(Fang et al. 2018; Tan et al. 2011; Wang et al. 2016a; Wang et al. 2016c; Zhang et al. 2019b), uniaxial compressive strength (UCS)(Fang et al. 2018; Khanlari et al. 2014; Momeni et al. 2016; Wang et al. 2016a; Wang et al. 2016c; Yavuz 2010; Zhang et al. 2019b), Brazilian tensile strength (BTS)(Altindag et al. 2004; Jamshidi et al. 2013; Jia et al. 2015; Zhang et al. 2019c), point load strength (PLS)(Altindag et al. 2004; Jamshidi et al. 2013), dynamic uniaxial compressive strength (UCS_d)(Ke et al. 2018; Li et al. 2018; Ma et al. 2018; Wang et al. 2016a; Wang et al. 2016c; Weng et al. 2020; Zhang et al. 2019b) and dynamic tensile strength (BTS_d)(Liu et al. 2018; Weng et al. 2020) all decrease with the quantity of F&T weathering cycles increases, but to different extents. In order to reveal the change laws in these mechanical parameters with the quantity of F&T weathering cycles, a sequences of regression analysis models(Bayram 2012; İnce and Fener 2016) and exponential decay models(Altindag et al. 2004; GAO et al. 2019; Ghobadi et al. 2016; Jamshidi et al. 2013; Mutlutürk et al. 2004) have been proposed based on the relationships between these mechanical parameters and the quantity of F&T weathering cycles. In addition, Liu et al.(Liu et al. 2015) regarded F&T weathering cycles as a kind of fatigue damage, and a fatigue damage model of rocks after undergoing F&T weathering cycles was established. A prediction model of UCS of rocks after undergoing F&T weathering cycles was obtained based on this fatigue damage model. Gao et al.(Gao et al. 2020) established the UCS evolution model of frozen-thawed rocks based on energy evolution characteristics of rock failure. However, these research findings mainly

66 focused on rock uniaxial mechanical properties of rocks after undergoing F&T weathering
67 cycles, which did not consider the impact of confining pressure on mechanical properties of
68 rocks after undergoing F&T weathering process. There is no doubt that the actual rock mass
69 engineering is always in a certain stress field(Wang et al. 2019; Zhang et al. 2019a). To be
70 closer to the actual engineering, it is necessary to study triaxial mechanical properties of rocks
71 after undergoing F&T weathering cycles.
72 Recently, scholars have increasingly studied triaxial mechanical properties of rocks after
73 undergoing F&T weathering cycles. Tan et al.(Tan et al. 2011) used granite as the research
74 object to investigate the impact of the quantity of F&T weathering cycles on uniaxial and
75 triaxial mechanical properties according to uniaxial compression tests (UCT) and triaxial
76 compression tests (TCT) after granite specimens being underwent F&T weathering process.
77 They found that both UCS and TCS decrease exponentially with the quantity of F&T
78 weathering cycles increases, as did the elastic modulus and cohesion. The relationships
79 between these mechanical properties and the quantity of F&T weathering cycles were built
80 according to an exponential function. Wang et al.(Wang et al. 2019) and Hosseini and
81 Khodayari(Hosseini and Khodayari 2019) also carried out similar studies taking sandstone as
82 the research object, and the research results both in accordance with those of Tan et al(Tan et
83 al. 2011). In addition, Hosseini and Khodayari(Hosseini and Khodayari 2019) also found that
84 the rate of reduction in the TCS was less than that of the UCS at the equivalent quantity of F&T
85 weathering cycles, and the higher the confining pressure is, the lower the rate of reduction is.
86 It is evident that the confining pressure have significant impact on TCS of rocks after
87 undergoing F&T weathering cycles. To this end, Fu et al.(Fu et al. 2018) operated a sequences
88 of TCT after transversely isotropic rocks being underwent F&T weathering process, and they
89 found that the quantity of F&T weathering cycles, bedding plane orientation and confining
90 pressure have significant impact on TCS of slate. A TCS prediction model for transversely
91 isotropic rocks after being underwent F&T weathering process was proposed based on the
92 single discontinuity theory and the functional relationships between cohesion and internal
93 friction angle and the quantity of F&T weathering cycles. Seyed Mousavi et al.(Seyed Mousavi
94 et al. 2019) also carried out similar studies taking calc-schist rock specimens as the research
95 objects. Finally, an empirical expression among the TCS, the quantity of F&T weathering
96 cycles and confining pressure was obtained according to experimental results and the
97 prediction model suggested by Fu et al.(Fu et al. 2018) Although the prediction model proposed
98 by Fu et al.(Fu et al. 2018) could effectively reflect the coupling impact of the quantity of F&T
99 weathering cycles and confining pressure on TCS of rocks after being underwent F&T

weathering process, however, this prediction model is based on transversely isotropic rocks and its applicability is not strong. Therefore, it is necessary to establish a more applicable strength evolution model to reveal the coupling impact of the quantity of F&T weathering cycles and confining pressure on TCS of rocks after being underwent F&T weathering process. In addition, these above-mentioned studies mainly focused on investigating strength deterioration characteristics of rocks after undergoing F&T weathering process, which did not deeply investigated deformation behaviours of rocks, especially the coupling impact of the quantity of F&T weathering cycles and confining pressure on deformation behaviours of rocks during the entire loading procedure.

In this study, saturated sandstone specimens were first subjected to different quantities of F&T weathering cycles, and change laws in the T_2 spectrum distribution curves of sandstone specimens before and after F&T weathering cycles were investigated. UCT and TCT of sandstone specimens after undergoing different quantities of F&T weathering cycles were conducted to obtain the UCS and TCS and the corresponding stress-strain curves. The coupling impact of the quantity of F&T weathering cycles and confining pressure on deformation behaviours of rocks were investigated. A novel strength evolution model considering the coupling impact of the quantity of F&T weathering cycles and confining pressure on TCS of rocks after undergoing F&T weathering process was established, and the proposed strength evolution model was cross-verified with experimental data from the published literature.

2 Experimental materials and methods

2.1 Rock specimen preparation

In this paper, rock specimens were sandstone which taken from the Jiama open pit copper mine located in the Tibet autonomous region of China. The sampling site as shown in Fig. 1a. Fig. 1b shows the distribution map for frozen soil of China. It can be seen Fig. 1b that the sampling site is on the boundary between the permafrost regions and seasonal frozen regions, therefore, the rock has been underwent the repeated F&T weathering cycles. Table 1 shows the mineral composition of sandstone, which obtained by X-ray diffraction (XRD) technique.

Table 1 Mineral composition of sandstone specimens

Rock type	Mineral composition			
	Quartz (%)	Kaolinite (%)	Feldspar (%)	Mica (%)
Sandstone	88.14	7.44	3.05	1.37

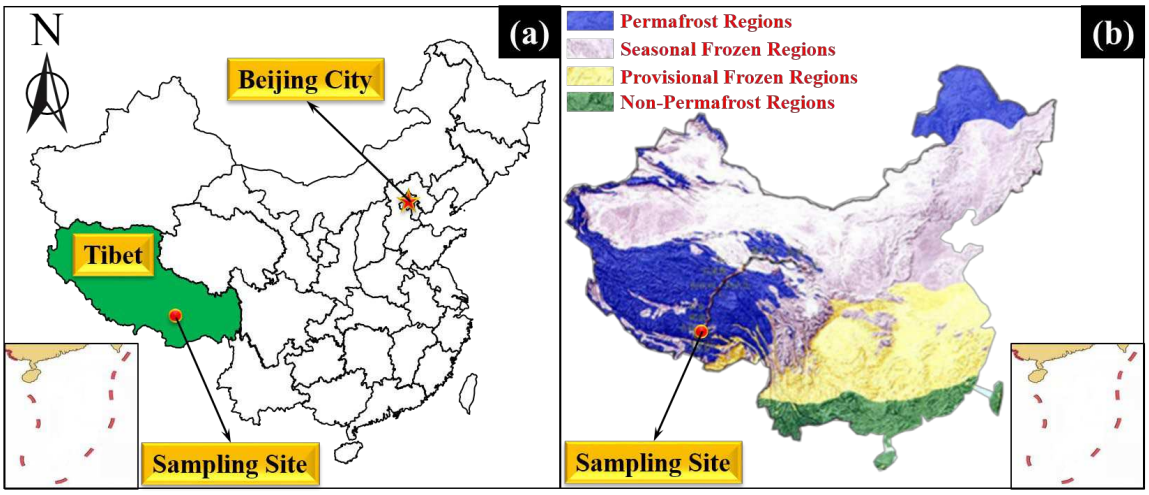

Fig. 1 Location of the sampling site: (a) location of the Jiama open pit cooper mine; and (b) distribution map for frozen soil of China.

Based on the method suggested by the ISRM, all rock specimens are processed into cylinder with a diameter of 50 millimeter, and ensure that the flatness of end surfaces was less than 0.05 millimeter(Ulusay 2015). Careful preparations ensured that the maximum deviations of the diameter and height were less than 0.30 millimeter, and the vertical variance was less than 0.25°(Ulusay 2015). In this study, fifteen and sixty rock specimens were used in UCT and TCT, respectively, and the length/diameter ratio of rock specimens is 2.0(Ulusay 2015). These specimens were divided into five groups (labelled A, B, C, D and E), and each group comprised fifteen rock specimens (labelled 1, 2 … 14, 15). The sandstone specimens from group A, B, C, D and E were treated in 0cycle, 10cycles, 20cycles, 30cycles and 40cycles, respectively. As shown in Fig. 2a, the sandstone specimens were labelled 1-3 in each group were used for UCT. The confining pressures are 3, 6, 9 and 12 MPa in the TCT, corresponding to the sandstone specimens were labelled 4-6, 7-9, 10-12 and 13-15 in each group, as shown in Fig. 2b.

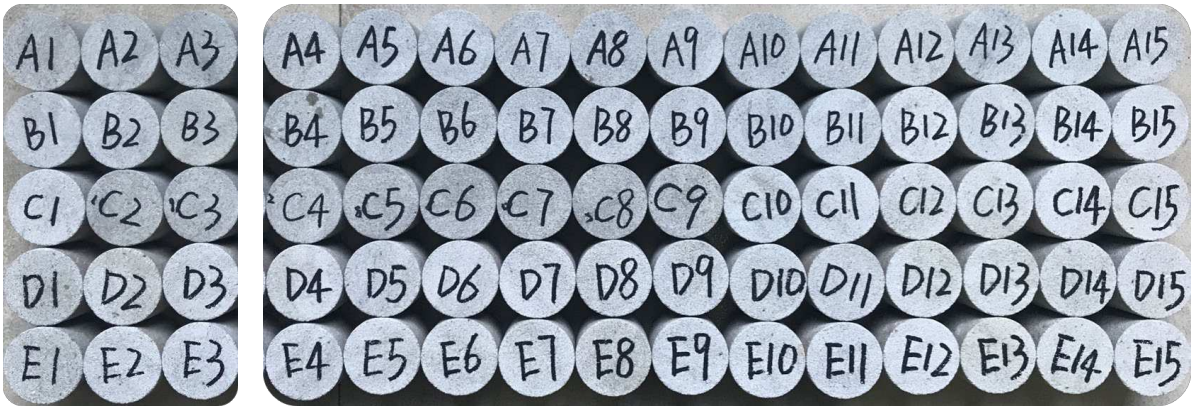

(a) (b)

Fig. 2 Rock Specimens: (a) specimens for uniaxial compression tests; and (b) specimens for triaxial compression tests.

2.2 Test procedures and experimental apparatus

All sandstone specimens were divided into five groups and dried in an oven for 48 hours at 65ºC. The sandstone specimens without undergoing F&T weathering cycles were used directly to for UCT and TCT. The other sandstone specimens were placed in a vacuum pump with a pressure of 0.1 MPa for four hours, and next soaked in distilled water for twenty-four hours. The saturated specimens then went through specified quantity of F&T weathering cycles in a TDS-300 automatic F&T testing machine (as shown in Fig. 3a). When the quantity of F&T weathering cycles came to the specified quantities, the corresponding sandstone specimens were removed, and UCT and TCT were operated on an MTS815 electrohydraulic servo-controlled rock testing machine (as shown in Fig. 3c).

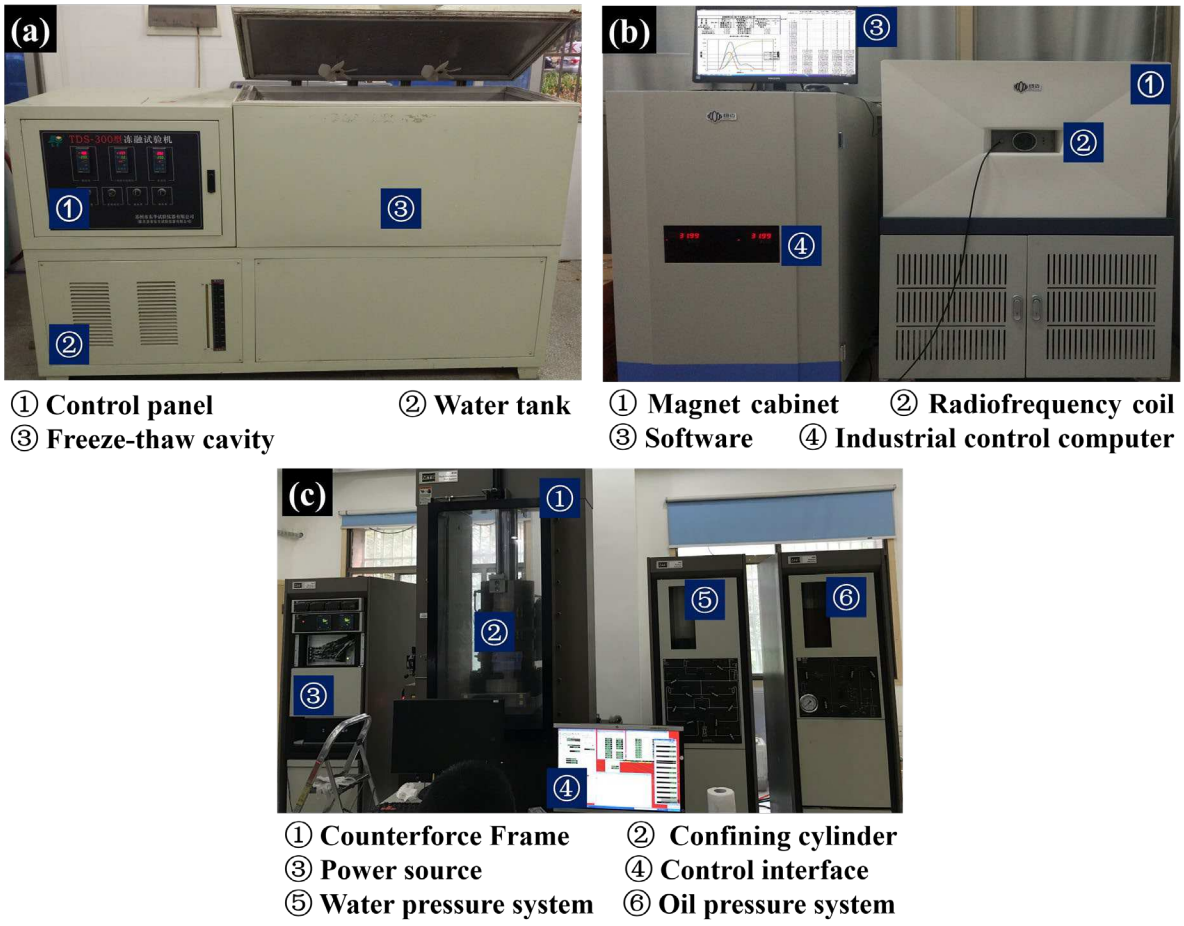

Fig. 3 Experiment instrument: (a) TDS-300 automatic freeze-thaw test machine; (b) MesoMR23-060H-I NMR system; and (c) MTS815 electrohydraulic servo-controlled rock testing machine.

2.3 F&T weathering cycles tests

Designed based on the local climate of the sampling site, one F&T weathering cycle in our tests included freezing the saturated rock specimens at -20°C for four hours and then thawing in water at +20°C for four hours. The temperature variation curve of the F&T

weathering process is shown in Fig. 4. In this study, four groups of sandstone specimens were subjected to F&T weathering tests corresponding to 10cycles, 20cycles, 30cycles and 40cycles. In order to reveal evolution characteristics of F&T damage, the MesoMR23-060H-I NMR system (as shown in Fig. 3b) was used to conduct Nuclear magnetic resonance (NMR) tests to obtain T_2 spectrum distribution curves before and after the F&T weathering cycles(Gao et al. 2016; Li et al. 2016; Li et al. 2012; Liu et al. 2020; Shen et al. 2020; Sun et al. 2020; Wang et al. 2020).

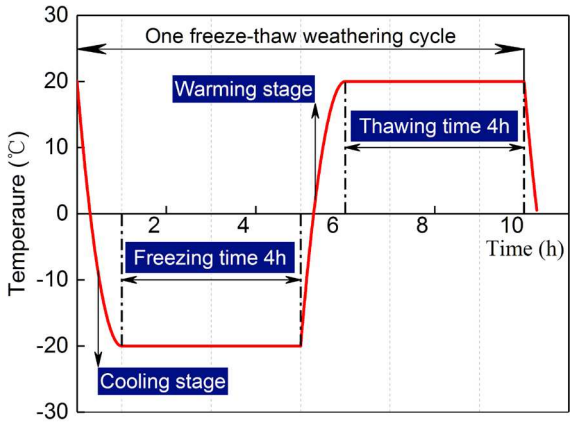

Fig. 4 Temperature variation curves of one F&T weathering cycle.

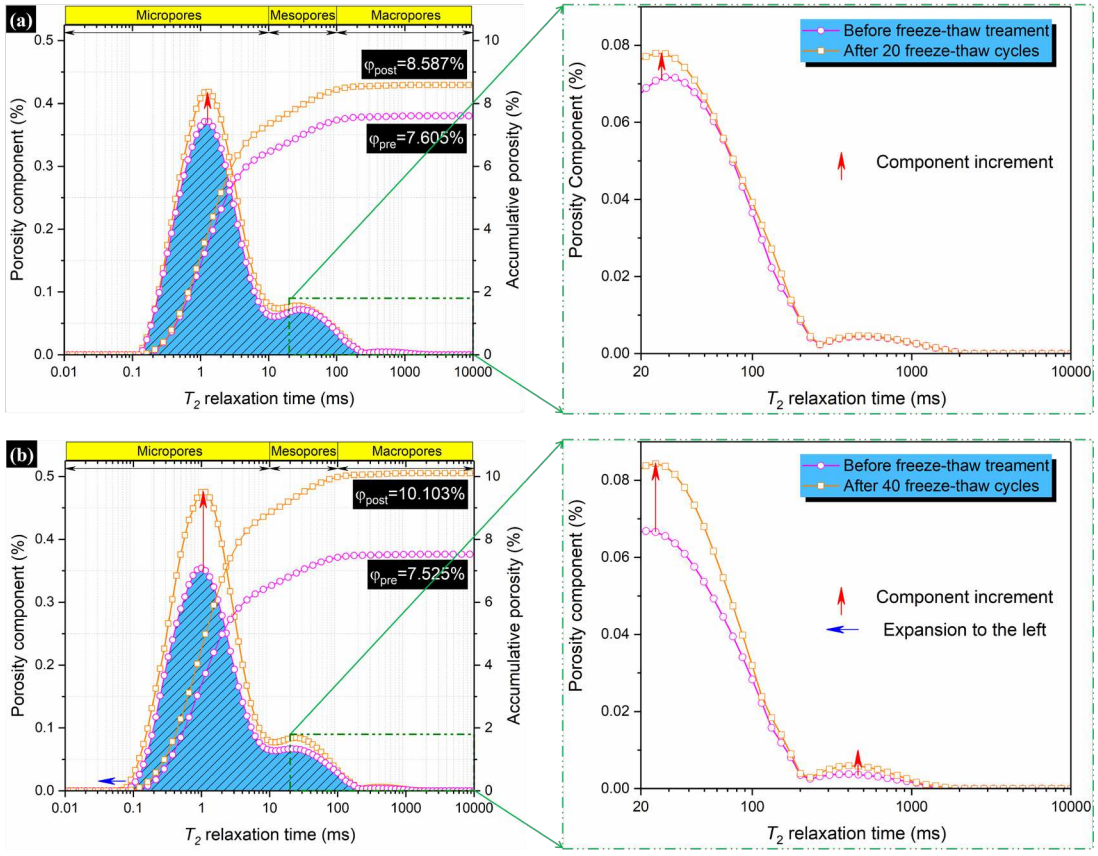

Fig. 5 T_2 spectrum distribution curves of sandstone specimens at different quantities of F&T weathering cycles: (a) 20 F&T weathering cycles and (b) 40 F&T weathering cycles.

Fig. 5 displays T_2 spectrum distribution curves of sandstone specimens before and after 20 (as shown in Fig. 5a) and 40 (as shown in Fig. 5b) F&T weathering cycles. In T_2 spectrum distribution curves, the T_2 relaxation time (horizontal axis) is a measurement of the internal pore sizes, and the porosity component (vertical axis) is the proportion of the corresponding pore sizes(Li et al. 2018). As can be seen from Fig. 5a, after the sandstone specimens being underwent 20cycles, the peak values of T_2 spectrum distribution curve increases, indicating the sizes of the internal pores increases. As shown in Fig. 5b, when the sandstone specimens after undergoing 40cycles, the increases of peak values are even more significant. In addition, the expansion of the curve to the left suggests that the sizes of some small pores increase. This demonstrates that in the early stage of F&T weathering cycles, the original internal pores and microcracks are constantly developing. With the increase of quantity of F&T weathering cycles, in the later stage of F&T weathering cycles, in addition to the expansion of original internal pores and the constant extension of microcracks, new pores and microcracks are generated, i.e., with the increase of quantity of F&T weathering cycles, the accumulated damage inner sandstone specimens constantly increases.

2.4 Uniaxial and triaxial compression tests

UCT and TCT were conducted on an MTS815 electrohydraulic servo-controlled rock testing machine. The axial and circumferential extensometers were used in our experiment to measure the axial and lateral strains. In our experiment, the displacement-control loading mode was used and the loading rate is 0.1 mm/min. The measured UCS and TCS of sandstone specimens are listed in Table 2.

Table 2 Uniaxial and triaxial compression test results of sandstone specimens after undergoing different quantities of F&T weathering cycles

Quantity of F&T weathering cycles	Confining pressure (MPa)	Specimen ID	Diameter (mm)	Height (mm)	Peak compressive strength (MPa)	
					Tested value	Average value
0	0	A1	48.54	100.26	26.94	27.50
		A2	49.12	100.28	27.51	
		A3	48.96	99.88	28.05	
	3	A4	49.06	100.02	48.78	49.34
		A5	49.14	99.84	47.99	
		A6	49.02	100.16	51.26	
	6	A7	48.94	100.10	62.87	63.28
		A8	49.06	100.14	64.75	
		A9	49.00	100.28	62.23	
	9	A10	48.74	100.22	72.12	74.61
		A11	48.88	100.08	75.46	
		A12	48.96	100.20	76.25	
	12	A13	49.48	99.84	83.76	85.08
		A14	48.94	99.88	85.24	
		A15	48.04	100.16	86.25	

		B1	49.12	100.02	25.60	
	0	B2	49.46	100.02	24.11	24.38
		B3	48.96	99.84	23.44	
		B4	48.86	100.04	44.88	
	3	B5	48.74	100.28	45.58	44.58
		B6	48.56	100.06	43.28	
		B7	48.52	100.12	56.86	
10	6	B8	49.10	100.12	57.22	57.57
		B9	49.04	100.66	58.64	
		B10	49.02	100.18	70.33	
	9	B11	48.98	99.94	67.40	68.99
		B12	48.96	100.24	69.24	
		B13	49.14	99.94	81.88	
	12	B14	48.82	99.72	79.55	80.13
		B15	48.84	100.16	78.96	
		C1	49.04	100.02	19.68	
	0	C2	48.88	100.10	20.62	20.79
		C3	49.18	99.90	22.06	
		C4	48.96	100.24	39.12	
	3	C5	49.04	100.10	42.89	40.11
		C6	49.04	100.12	38.33	
		C7	49.08	100.18	52.11	
20	6	C8	48.76	99.82	54.48	53.25
		C9	48.52	100.22	53.15	
		C10	48.74	99.98	65.40	
	9	C11	48.70	99.86	64.06	64.24
		C12	49.12	100.14	63.25	
		C13	49.20	100.20	74.59	
	12	C14	49.78	99.86	72.66	74.28
		C15	48.88	99.96	75.58	
		D1	49.52	100.16	19.04	
	0	D2	48.84	99.88	18.2	18.17
		D3	49.04	100.02	17.26	
		D4	48.36	100.02	35.18	
	3	D5	49.12	99.78	38.97	36.47
		D6	48.76	100.06	35.26	
		D7	48.82	100.16	48.80	
30	6	D8	49.06	99.78	50.81	49.29
		D9	49.92	100.04	48.25	
		D10	48.80	99.86	58.28	
	9	D11	49.06	100.02	60.16	59.41
		D12	49.82	99.90	59.78	
		D13	49.02	100.22	66.62	
	12	D14	49.28	100.16	65.37	67.26
		D15	49.12	99.94	69.78	
		E1	48.84	99.84	15.88	
	0	E2	48.84	100.04	16.41	16.39
		E3	48.60	100.20	16.88	
		E4	49.02	100.18	33.06	
	3	E5	48.86	99.88	31.78	32.84
		E6	48.68	100.30	33.68	
		E7	48.76	99.84	45.82	
40	6	E8	48.98	100.08	42.75	43.94
		E9	48.68	100.14	43.25	
		E10	48.96	10.14	52.73	
	9	E11	48.88	100.02	49.9	52.29
		E12	49.08	100.14	54.25	
		E13	48.92	100.18	61.77	
	12	E14	49.16	99.92	59.38	61.13
		E15	48.90	100.20	62.25	

3 Experimental results and analysis

3.1 Uniaxial mechanical properties variation characteristics of sandstone after undergoing F&T weathering cycles

3.1.1 Stress-strain curve

Fig. 6 displays stress-strain curves of sandstone specimens after undergoing different quantities of F&T weathering cycles under uniaxial compression conditions. All stress-strain curves have the same variation patterns, stress-strain curves both could be separated into five stages during the whole load process, that is, compaction stage, elastic deformation stage, yield stage, failure stage and strain softening stage. As the quantity of F&T weathering cycles increases, the stress-strain curve shows three obvious features: (1) the compaction stage becomes longer, (2) the slope at the linear deformation stage decreases, as does the UCS, and (3) the stress dropping rate of the post-peak decreases. The main reason is that the length of the compaction stage and the slope of the linear deformation stage are proportional to the number of micro-defects inside the rock. Under F&T weathering process, water migration and transformation from water to ice causes micro-defects gradually develop, and the number of micro-defects increase as the increase of quantity of F&T weathering cycles. The main reason for the reduction of the stress dropping rate of the post-peak is that F&T weathering cycles cause cohesion between the particles to gradually decrease, which causes sandstone specimens become soft and the plasticity to increase.

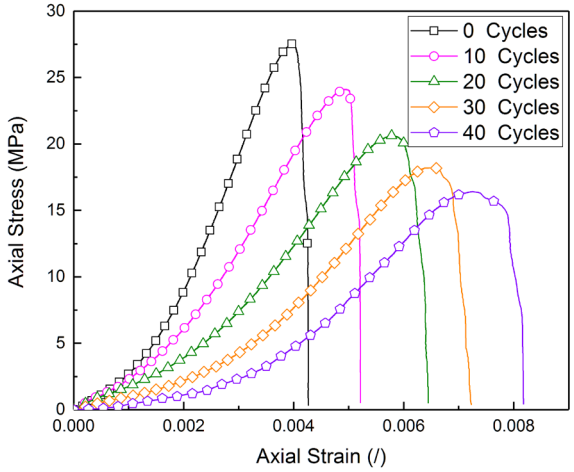

Fig. 6 Stress-strain curves of sandstone specimens after undergoing different quantities of F&T weathering cycles at uniaxial compression tests.

3.1.2 UCS

Fig 7 shows the changes in the UCS and its reduction ratio at different quantities of F&T weathering cycles. The reduction ratio of UCS is defined as follows:

$$\eta = \frac{\sigma_0 - \sigma_N}{\sigma_0} \times 100\% \quad (1)$$

where σ_0 is the UCS of sandstone specimens without any F&T weathering cycles; σ_N is the UCS of sandstone specimens after undergoing N quantity of F&T weathering cycles; and η is the reduction ratio of the UCS.

As shown in Fig. 7, compared with the original average UCS (27.50 MPa), the reduction ratios are 11.33% (24.38 MPa), 24.41% (20.79 MPa), 33.94% (18.17 MPa) and 40.40% (16.39 MPa), corresponding to 10cycles, 20cycles, 30cycls, and 40 cycles, respectively. The reason could be explained as follows: the water migration and transformation from water to ice under the F&T weathering process causes micro-defects gradually develop, and sandstone specimens become more fragmented. It is noticeable that the UCS exponentially decays with the quantity of F&T weathering cycles increases, similar to laws in the literature(Ghobadi et al. 2016; Jamshidi et al. 2013; Mutlutürk et al. 2004). The experimental data was fitted by the decay model suggested by Mutlutürk et al.(Mutlutürk et al. 2004), and the decay model is defined as follows:

$$I_N = I_0 e^{-\lambda N} \quad (2)$$

where I is the rock integrity; λ is the decay coefficient; and N is the quantity of F&T weathering cycles.

In this paper, the UCS was regarded as the rock integrity, therefore, the decay model becomes as follows:

$$\sigma_N = \sigma_0 e^{-\lambda N} \quad (3)$$

Fitting curves of our test are shown in Fig. 7. The model fits well with experimental data, and the fitting coefficient of determination (R^2) greater than 0.99.

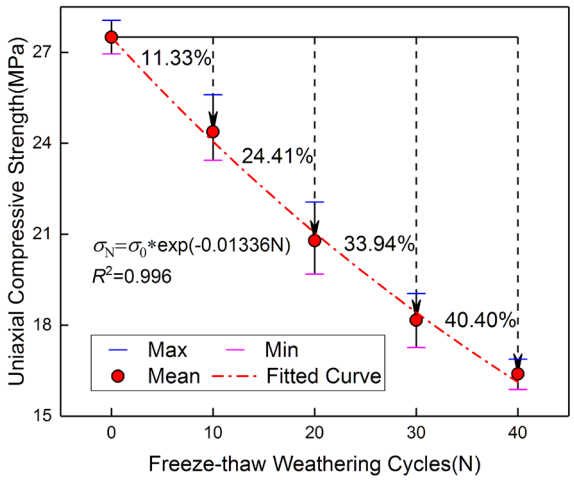

Fig. 7 UCS and its reduction ratio of sandstone specimens after undergoing different quantities of F&T weathering cycles.

3.1.3 Failure modes

Fig. 8 shows failure modes of the sandstone specimens after undergoing different quantities of F&T weathering cycles at uniaxial compression conditions. The failure mode is single incline plane shear failure when sandstone specimens without undergoing F&T weathering cycles. The failure modes become tension-shear comprehensive failure and splitting failure with the quantity of F&T weathering cycles increases. Tension-shear comprehensive failure occurs in the sandstone specimens after undergoing 10cycles and 20 cycles, and sandstone specimens are fragmented. Splitting failure occurs in sandstone specimens when the quantity of F&T weathering cycles are 30 and 40. The increase of number of macroscopic cracks on the surfaces of sandstone specimens, and sandstone specimens become more fragmented. The reason of failure modes change with the quantity of F&T weathering cycles is that the F&T weathering process causes micro-defects to gradually develop inside the sandstone specimens, which causes cracks to be more likely to expand in the axial direction under uniaxial compression conditions.

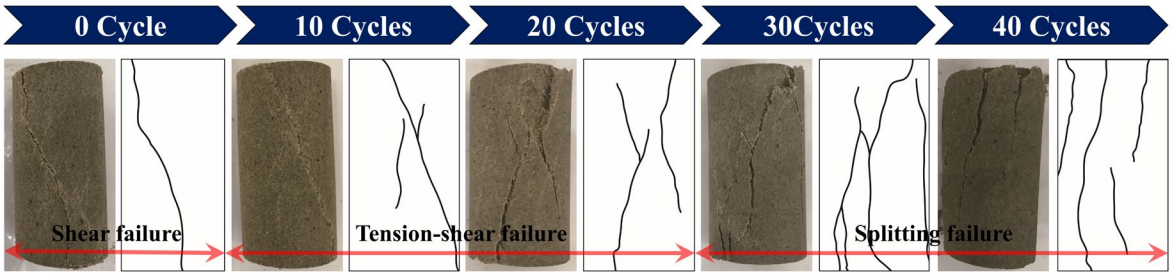

Fig. 8 Failure modes of sandstone specimens after undergoing different quantities of F&T weathering cycles at uniaxial compression tests.

3.2 Triaxial mechanical properties variation characteristics of sandstone after undergoing F&T weathering cycles

3.2.1 Stress-strain curve

Fig. 9 displays stress-strain curves of sandstone specimens after undergoing different quantities of F&T weathering cycles under different confining pressures. Compared with stress-strain curves of sandstone specimens after undergoing different quantities of F&T weathering cycles under uniaxial compression conditions, all stress-strain curves have obvious residual strength characteristics. In addition to, variation characteristics of stress-strain curves are similar under different confining pressures with the quantity of F&T weathering cycles increases. All stress-strain curves both could be separated into six stages: compaction stage, elastic deformation stage, yield stage, failure stage, strain softening stage and residual strength

stage. When the confining pressure is a constant, with the increase of quantity of F&T weathering cycles, except for the residual strength gradually decreases, the other variation characteristics are similar to those at uniaxial compression conditions, that is, (1) the compaction stage becomes longer, (2) the slope at the linear deformation stage decreases, as does the TCS, and (3) the stress drop rate in the post-peak stress decreases. The main reason for these characteristics are the same as that under uniaxial compression conditions.

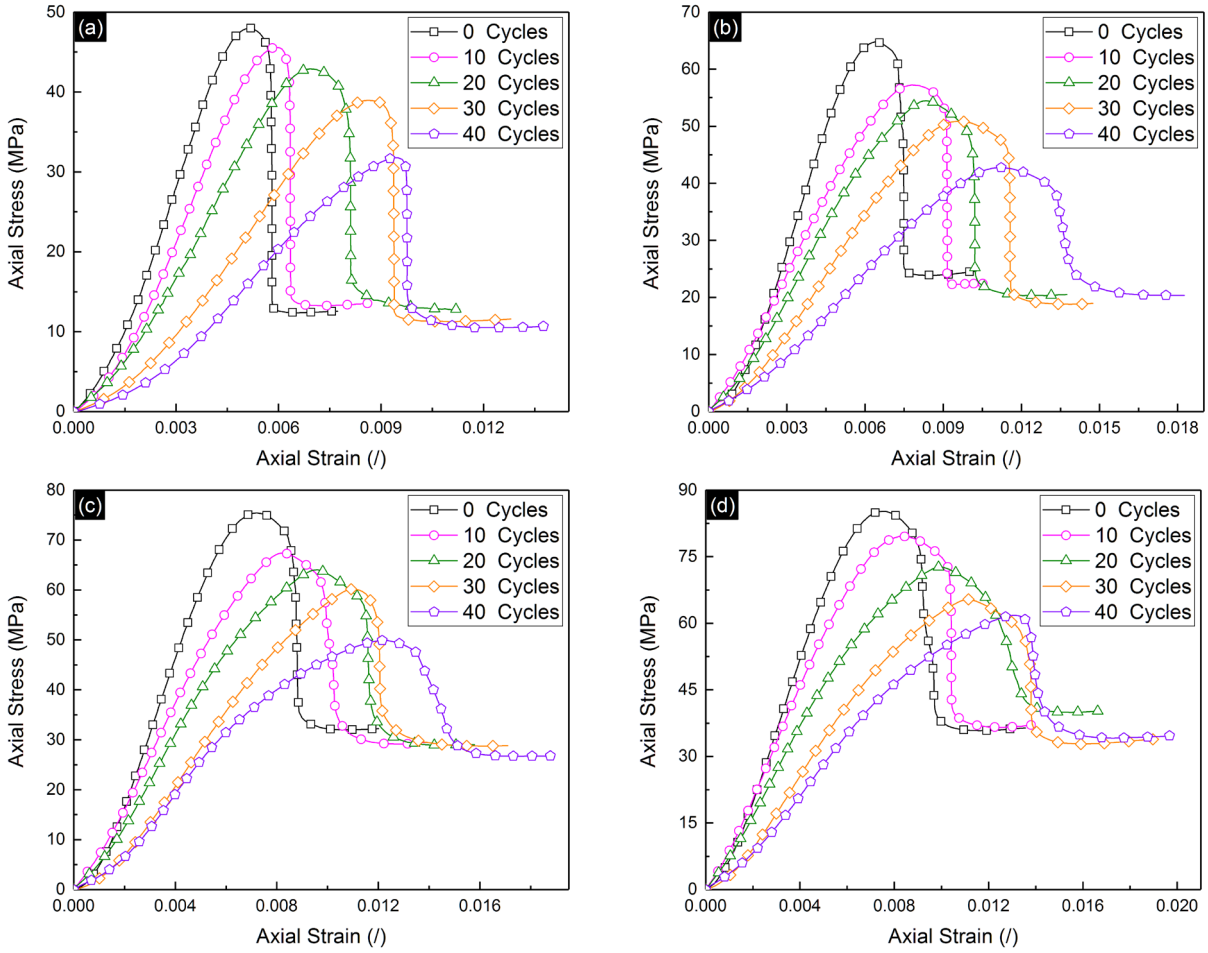

Fig. 9 Stress-strain curves of sandstone specimens after undergoing different quantities of F&T weathering cycles under triaxial compression tests: (a) 3 MPa; (b) 6 MPa; (c) 9 MPa; and (d) 12MPa.

Fig. 10 displays stress-strain curves of sandstone specimens after undergoing 20 F&T weathering cycles at different confining pressures. With the increase of confining pressure, stress-strain curves have four obvious features: (1) the compaction stage becomes shorter, (2) the slope at the linear deformation stage increases, as does the TCS, (3) the stress dropping ratio of the post-peak decreases, and (4) the residual strength increases. The main reason is that the length of the compaction stage and the slope of the linear deformation stage are proportional to the number of micro-defects inner the rock. Under the confining pressure, micro-defects inner the rock caused by the F&T weathering process are pre-compression, which causing the

decrease of number of micro-defects, and the higher the confining pressure is, the larger the number of micro-defects that are pre-compression is. The main reason for the decrease of stress dropping ratio of the post-peak and the increase of residual strength is that the confining pressure could make the post-peak deformation behaviour of rocks transition from brittleness to plasticity(Rummel and Fairhurst 1970; Yao et al. 2016; Zhang et al. 2008; Zhao et al. 2018).

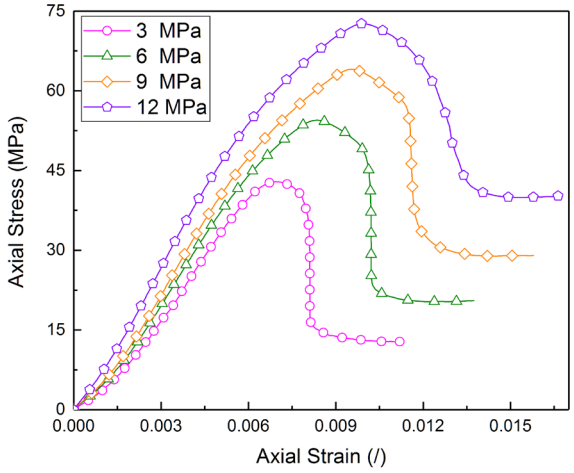

Fig. 10 Stress-strain curves of sandstone specimens at different confining pressures (20 F&T weathering cycles).

These variation characteristics indicate that the impact of the quantity of F&T weathering cycles on pre-peak deformation behaviour and residual strength are opposite confining pressure, and post-peak deformation behaviours are similar to confining pressure.

3.2.2 TCS

Fig. 11 displays the relationship between the TCS and its reduction ratio and the quantity of F&T weathering cycles at different confining pressures. It can be seen that the TCS decrease as the increase of quantity of F&T weathering cycles when the confining pressure is a constant, similar to laws in the uniaxial compression conditions. Compared with the original average TCS, the reduction ratios are 9.55%, 18.71%, 26.09% and 33.45%, corresponding to 10cycles, 20cycles, 30cycles, and 40cycles, respectively, when the confining pressure is 3 MPa; the reduction ratios are 9.02%, 15.86%, 22.12% and 30.57%, corresponding to 10cycles, 20cycles, 30cycles, and 40cycles, respectively, when the confining pressure is 6 MPa; the reduction ratios are 7.53%, 13.90%, 20.38% and 29.91%, corresponding to 10cycles, 20cycles, 30cycles, and 40cycles, respectively, when the confining pressure is 9 MPa; the reduction ratios are 5.82%, 12.70%, 20.95% and 30.57%, corresponding to 10cycles, 20cycles, 30cycles, and 40cycles, respectively, when the confining pressure is 12 MPa. At different confining pressures, variation characteristics between TCS of sandstone specimens and the quantity of F&T cycles are similar to UCS. Therefore, the experimental data could be used the model suggested by Mutlutürk et

al.(Mutlutürk et al. 2004) to fit, and fitting results of our tests are shown in Fig. 11. The model fit well with experimental data, and the fitting coefficient of determination (R^2) greater than 0.98. The decay coefficient are 0.01018, 0.00881, 0.00819 and 0.00778, corresponding to 3, 6, 9 and 12 MPa, respectively. The results indicate that the decay coefficient decrease with the confining pressure increases, and the higher the confining pressure is, the larger the reduction of in the decay coefficient is. Therefore, the TCS of sandstone after undergoing F&T weathering process is obviously impacted by confining pressure. To further study the impact of confining pressure on TCS of sandstone after undergoing F&T weathering process, referring to the definition of the dynamic increase factor(Cadoni 2010; Wang et al. 2016b). The confining pressure increase factor (CPIF) could be defined as TCS/UCS.

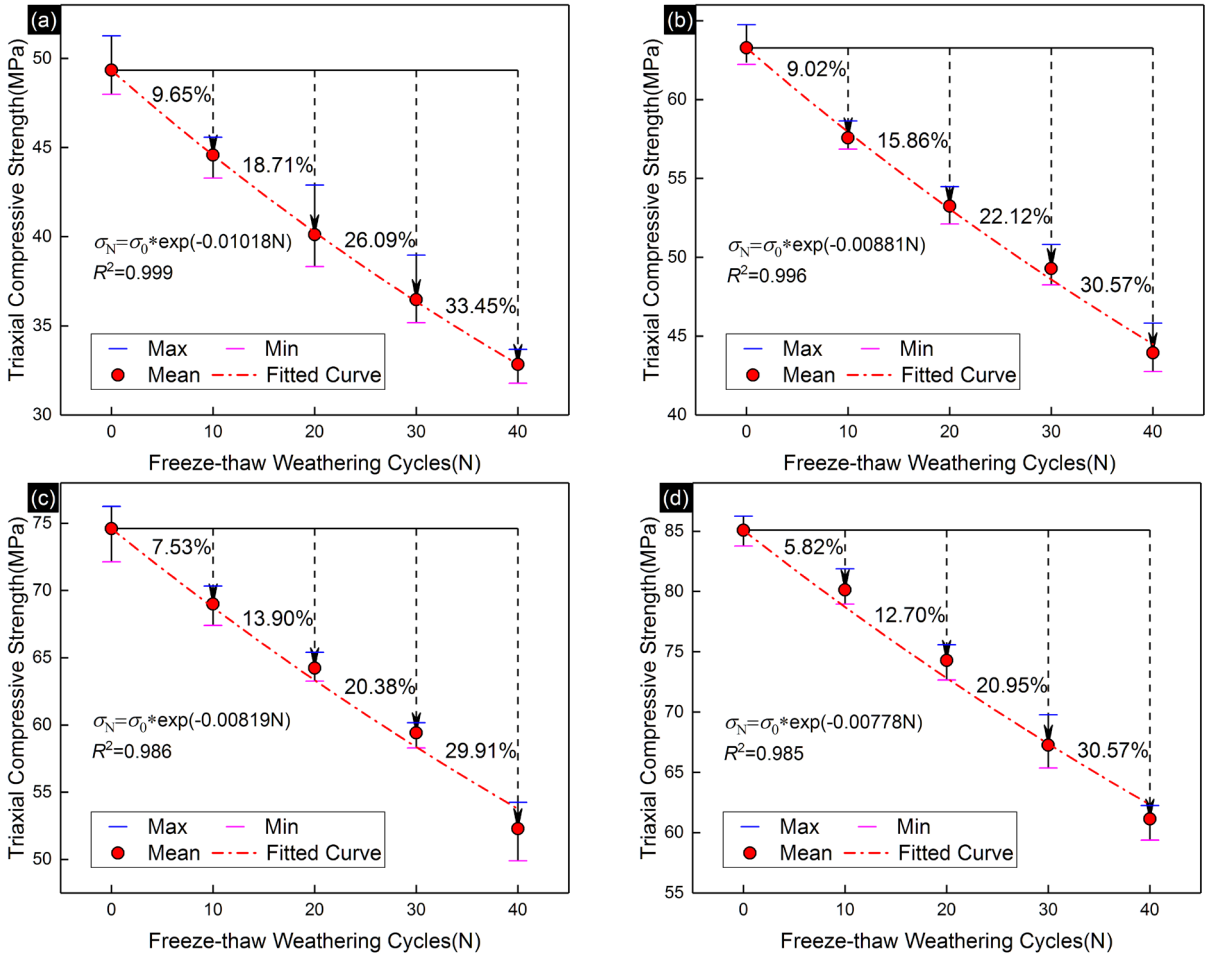

Fig. 11 TCS and its reduction ratio of sandstone specimens after undergoing different quantities of F&T weathering cycles: (a) 3 MPa; (b) 6 MPa; (c) 9 MPa; (d) 12 MPa.

Fig. 12 displays CPIF curves of sandstone specimens after undergoing different quantities of F&T weathering cycles at different confining pressures. As shown in Fig. 12, variation characteristics of CPIF curves are similar under different confining pressures with the quantity of F&T weathering cycles increases, that is, the CPIF increase with the quantity of F&T

weathering cycles increases. However, the higher the confining pressure is, the larger the increase amplitude of the CPIF is. For example, when the confining pressure is 3 MPa, the value of the CPIF is 1.79 without F&T weathering cycles, the CPIF is 2.31 after sandstone being underwent F&T weathering cycles, and the increase ratio is 28.97%; when the confining pressure is 12 MPa, the value of the CPIF is 3.09 without F&T weathering cycles, the CPIF is 4.83 after sandstone being underwent F&T weathering cycles, and the increase ratio is 56.27%. This indicate that sandstone specimens after undergoing more F&T weathering cycles are more sensitive to confining pressure.

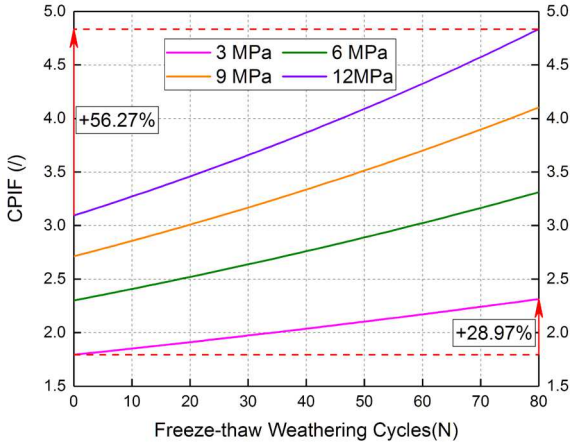

Fig. 12 Confining pressure increase factor curves at different confining pressures

These results demonstrate that the UCS of sandstone after undergoing F&T weathering process is mainly controlled by the quantity of F&T weathering cycles under uniaxial compression conditions. The TCS of sandstone after undergoing F&T weathering process is impacted by the quantity of F&T weathering cycles and confining pressure under triaxial compression conditions, and these two factors have completely opposite impacts. The main reason is that water-ice phase and water migration under F&T weathering cycles cause micro-defects to gradually develop inside sandstone specimens, which induces F&T damage. However, under confining pressure conditions, some micro-defects inside sandstone specimens have been closed, which lessens the damage induced by F&T weathering process. Therefore, for the slope engineering of open-pit mine in cold areas, application of the anchor reinforcement technology to provide prestress could lessen the damage induced by F&T weathering process and improve the stability of the slope.

3.2.3 Failure modes

Under different quantities of F&T weathering cycles, failure modes of sandstone specimens have same evolution characteristics with change of confining pressure. Therefore, Fig. 13 only shows failure modes under different confining pressures after sandstone specimens

being underwent 20 F&T weathering cycles. As shown in Fig. 13, under different confining pressures, failure modes of sandstone specimens both are single inclined plane shear failure, however, the length of the shear failure plane becomes shorter with the increase of confining pressure. The main reason is that the lateral deformation is limited under the confining pressure, so sandstone specimens only exhibit single inclined plane shear failure. In addition, the higher the confining pressure is, the more severe the limiting effect is, so the length of the shear failure plane becomes shorter with the increase of confining pressure.

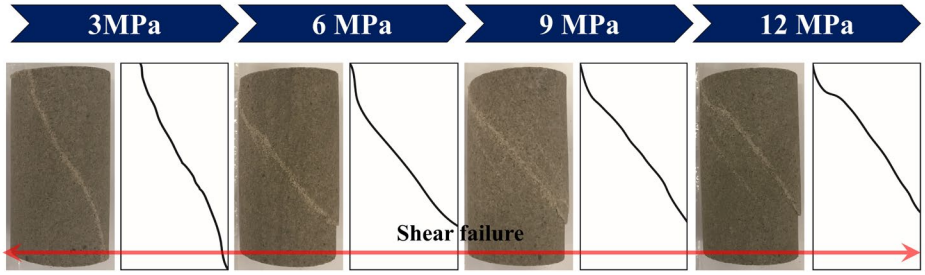

Fig. 13 Failure modes of sandstone specimens at different confining pressures (20 F&T weathering cycles).

4 Strength evolution model of rock specimens considering the freeze-thaw weathering process and confining pressure

The experimental results demonstrate that the TCS of rocks after undergoing F&T weathering process is impacted by the quantity of F&T weathering cycles and confining pressure under triaxial compression conditions. The model suggested by Mutlutürk et al. could only describe the change in the peak compressive strength of rocks after undergoing F&T weathering process at a specific confining pressure, which not considering the coupling impact of the quantity of F&T weathering cycles and confining pressure. Therefore, it is necessary to establish a novel model that could reflect evolution laws of TCS of rocks after undergoing F&T weathering process. The impact of confining pressure on TCS could be described by rock strength criterion. Hoek-Brown strength criterion proposed by Hoek-Brown could describe the failure of broken rock mass. The expression of Hoek-Brown strength criterion is as follows(Hoek and Brown 1997; Hoek et al. 2002):

$$\sigma_1 = \sigma_3 + \sqrt{m_i \sigma_{ci} \sigma_3 + \sigma_{ci}^2} \tag{4}$$

where σ_{ci} is the UCS; σ_1 is the TCS; m_i is the material constant; and σ_3 is the confining pressure.

Under F&T weathering process, the water migration and transformation from water to ice induces micro-defects to gradually develop, which causes the rock specimens become more fragmented. Therefore, Hoek-Brown strength criterion could be adopted to describe the impact of the confining pressure on the TCS of rocks after undergoing F&T weathering process.

σ_1 and confining pressure σ_3 could be simplified into a quadratic function expression. Based on this simplified relationship and the model suggested by Mutlutürk et al., this paper proposed a novel strength evolution model to describe the coupling impact of the quantity of F&T weathering cycles and confining pressure on TCS. The expression of the strength evolution model is as follows:

$$\sigma_1 = \left(a + b\sigma_3 + c\sigma_3^2\right)\exp\left[\left(d + e\sigma_3 + f\sigma_3^2\right)\mathrm{N}\right] \tag{5}$$

where a, b, c, d, e and f are fitting parameters determined by properties of rocks.

According to Eq. (5), MATLAB was adopted to fit experimental data of TCS of sandstone specimens after undergoing different quantities of F&T weathering cycles and different confining pressures, the fitting surface is shown in Fig. 14 and fitting parameters are shown in Table 3. As shown in Fig. 14 and Table 3, the fitting surface agrees well with the experimental data, and the correlation coefficient is up to 0.992, which indicates that the proposed model could effectively describe the coupling impact of the quantity of F&T weathering cycles and confining pressure on TCS of sandstone after undergoing F&T weathering process.

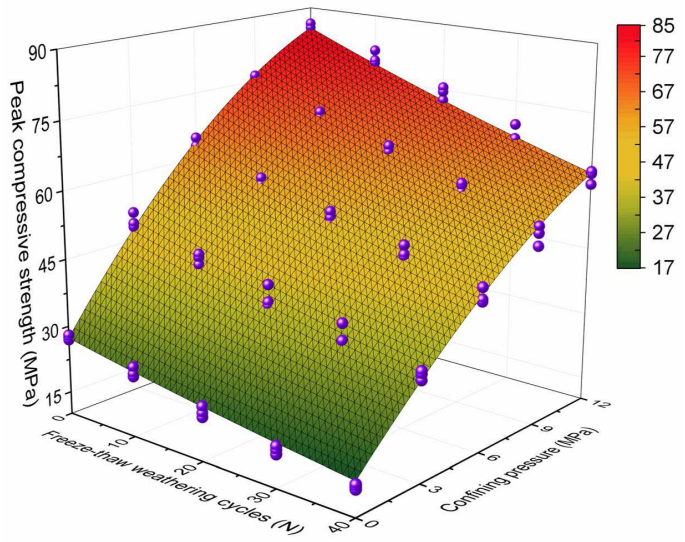

Fig. 14 Fitting results of TCS of sandstone specimens at different quantities of F&T weathering cycles and different confining pressures.

Table 3 Fitting parameters of strength evolution model of sandstone specimens

Fitting parameters	a	b	c	d	e	f	R^2
Value	27.358	7.412	-0.216	1.101×10^{-2}	3.257×10^{-4}	-6.043×10^{-6}	0.992

To further validate the rationality of proposed model in this paper, the Eq. (5) was adopted to fit the tested value from published literature(Fu et al. 2018; Hosseini and Khodayari 2019; Seyed Mousavi et al. 2019; Zhang et al. 2019a). The fitting surfaces are shown in Fig. 15, and fitting parameters are shown in Table 4. As shown in Fig. 15 and Table 4, fitting surfaces agree

well with the tested value, and all fitting correlation coefficients are above 0.95, which proves that the strength evolution model proposed in this paper is reasonable; in addition, this model has strong applicability.

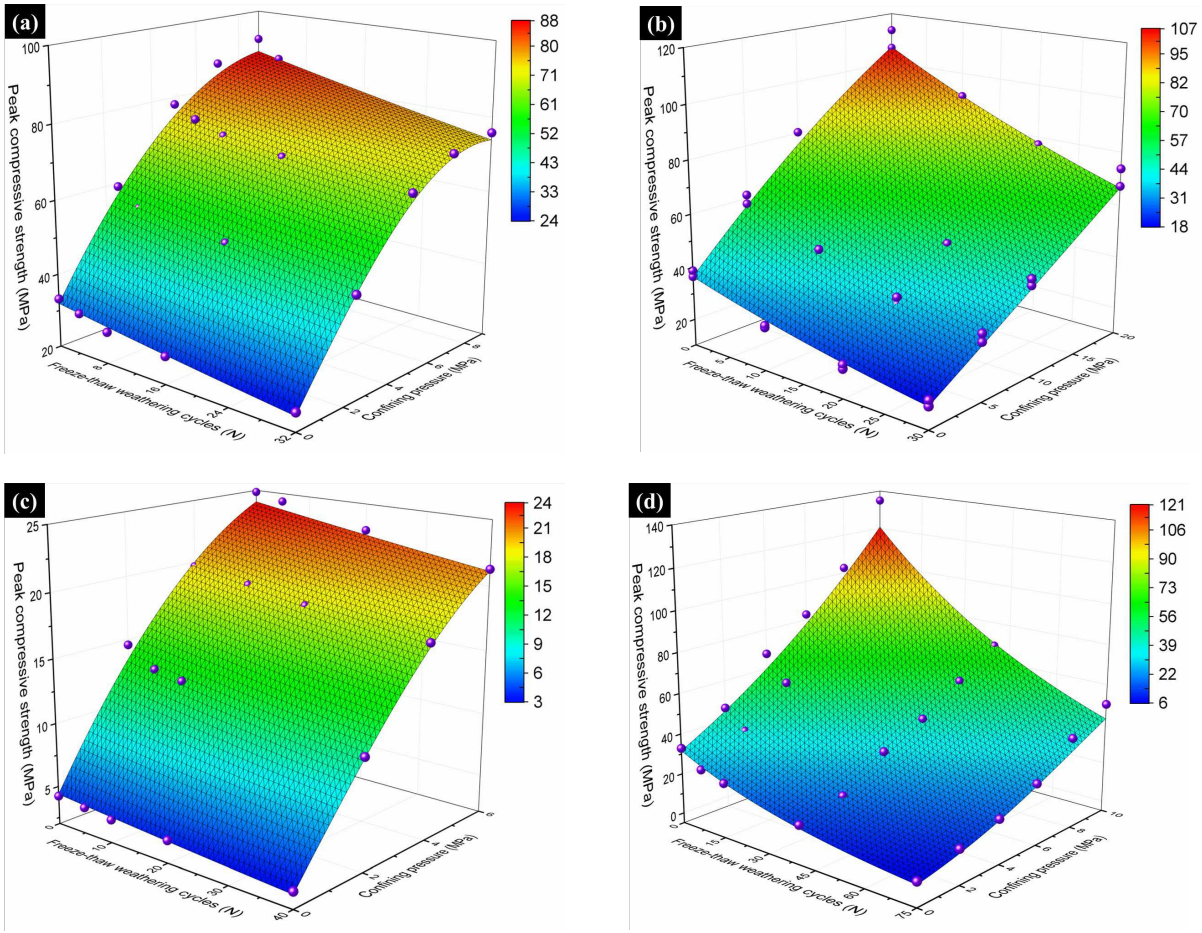

Fig. 15 Fitting results of TCS of rocks at different quantities of F&T weathering cycles and different confining pressures: (a) from (Hosseini and Khodayari, 2019);(b) from (Fu et al., 2018); (c) from (Zhang et al., 2019); and (d) from (Seyed Mousavi et al., 2019).

Table 4 Fitting parameters of strength evolution model of rock specimens from the published literature

Data source	Fitting parameters						
	a	*b*	*c*	*d*	*e*	*f*	R^2
From (Hosseini and Khodayari, 2019)	32.242	11.493	-0.580	9.190×10^{-3}	1.570×10^{-3}	-1.309×10^{-4}	0.988
From (Fu et al., 2018)	34.444	4.333	-0.042	2.314×10^{-2}	3.788×10^{-4}	-2.546×10^{-7}	0.977
From (Zhang et al., 2019).	4.387	5.155	-0.313	8.880×10^{-3}	1.500×10^{-3}	-9.298×10^{-5}	0.992
From (Seyed Mousavi et al., 2019)	31.680	5.907	0.299	-2.328×10^{-2}	1.810×10^{-3}	-8.714×10^{-5}	0.965

5 Conclusion

In this paper, the evolution characteristics of the F&T damage of sandstone was analysed based on NMR techniques. Uniaxial and triaxial compression tests of sandstone after undergoing different quantities of F&T weathering cycles were operated to investigate the coupling impact of the quantities of F&T weathering cycles and confining pressure on mechanical properties and failure modes. A novel strength evolution model was proposed to describe the coupling impact of the quantity of F&T weathering cycles and confining pressure on TCS of rocks after undergoing F&T weathering process. The following main conclusions could be drawn from this research:

(a) In the early stage of F&T weathering cycles, original internal pores and microcracks are constantly developing. With the quantity of F&T weathering cycles increases, in the later stage of F&T weathering cycles, besides the expansion of original internal pores and the constant extension of microcracks, new pores and microcracks are generated, i.e., , the accumulated damage inner sandstone specimens constantly increases with the quantity of F&T weathering cycles increases.

(b) The impact of the quantity of F&T weathering cycles on pre-peak deformation behaviours, peak compressive strength and residual strength are the opposite confining pressure, and post-peak deformation behaviours are similar to confining pressure. When the confining pressure is a constant, with the increase of quantity of F&T weathering cycles, the compaction stage becomes longer, and the slope at the linear deformation stage, the peak compressive strength, the residual strength and the stress dropping rate of the post-peak both decreases. When the quantity of F&T weathering cycles is a constant, with the increase of confining pressure, the compaction stage becomes shorter, and the slope at the linear deformation stage, the peak compressive strength and the residual strength both increases, but the stress dropping rate of the post-peak decreases.

(c) At uniaxial compression tests, the failure mode of sandstone specimens change with the quantity of F&T cycles increases. The failure mode is single inclined plane shear failure when sandstone specimens without undergoing F&T weathering cycles. In the early and later stages of F&T weathering cycles, failure modes become tension-shear comprehensive failure and splitting failure, respectively. At triaxial compression tests, the failure mode of sandstone specimens under different confining pressures both is single inclined plane shear failure, regardless of the quantity of F&T weathering cycles experienced. However, the length of the shear failure plane becomes shorter with the confining pressure increases.

(d) Variation characteristics of CPIF curves are similar under different confining pressures

with the quantity of F&T weathering cycles increases, that is, the CPIF increase with the quantity of F&T weathering cycles increases. However, the higher the confining pressure is, the larger the increase amplitude of the CPIF is. This indicate that sandstone specimens after undergoing more F&T weathering cycles are more sensitive to confining pressure.

(e) A novel strength evolution model that could describe the coupling impact of the quantity of F&T weathering cycles and confining pressure on TCS of rocks after undergoing F&T weathering process was proposed. The proposed model was cross-verified with tested value from the published literature. Fitting surfaces agree well with the tested value, and all fitting correlation coefficients are above 0.95, which proves that the strength evolution model proposed in this paper is reasonable; in addition, this model has strong applicability.

Acknowledgements

This work was supported by the National Natural Science Foundation of China (Grant No. 51774323), Hunan Provincial Natural Science Foundation of China (Grant No. 2020JJ4704 and 2020JJ4712) and the fundamental research funds for the central universities of Central South University, China (Grant No. 2021zzts0279).

Declaration of interests

The authors declare that they have no known competing financial interests or personal relationships that could have appeared to influence the work reported in this paper.

CRediT author statement

Xin Xiong: Conceptualization, Investigation, Methodology, Data Curation and Writing - Original Draft. Keping Zhou: Supervision, Funding acquisition and Conceptualization. Feng Gao: Data Curation, Funding acquisition and Writing - Review & Editing. Chun Yang: Investigation and Writing - Review & Editing. Jielin Li: Funding acquisition

References

Altindag R, Alyildiz IS, Onargan T (2004) Mechanical property degradation of ignimbrite subjected to recurrent freeze–thaw cycles International Journal of Rock Mechanics and Mining Sciences 41:1023-1028 doi:10.1016/j.ijrmms.2004.03.005

Bayram F (2012) Predicting mechanical strength loss of natural stones after freeze–thaw in cold regions Cold Regions Science and Technology 83-84:98-102 doi:10.1016/j.coldregions.2012.07.003

Cadoni E (2010) Dynamic Characterization of Orthogneiss Rock Subjected to Intermediate and High Strain Rates in Tension Rock Mechanics and Rock Engineering 43:667-676 doi:10.1007/s00603-010-0101-x

Fang X, Xu J, Wang P (2018) Compressive failure characteristics of yellow sandstone subjected to the

492 coupling effects of chemical corrosion and repeated freezing and thawing Engineering Geology
493 233:160-171 doi:10.1016/j.enggeo.2017.12.014
494 Fu H, Zhang J, Huang Z, Shi Y, Chen W (2018) A statistical model for predicting the triaxial compressive
495 strength of transversely isotropic rocks subjected to freeze–thaw cycling Cold Regions Science and
496 Technology 145:237-248 doi:10.1016/j.coldregions.2017.11.003
497 Gao F, Cao S, Zhou K, Lin Y, Zhu L (2020) Damage characteristics and energy-dissipation mechanism of
498 frozen–thawed sandstone subjected to loading Cold Regions Science and Technology 169
499 doi:10.1016/j.coldregions.2019.102920
500 Gao F, Wang Q, Deng H, Zhang J, Tian W, Ke B (2016) Coupled effects of chemical environments and
501 freeze–thaw cycles on damage characteristics of red sandstone Bulletin of Engineering Geology and
502 the Environment 76:1481-1490 doi:10.1007/s10064-016-0908-0
503 Gao F, Xiong X, Zhou K-p, Li J-l, Shi W-c (2019) Strength deterioration model of saturated sandstone under
504 freeze-thaw cycles Rock and Soil Mechanics 40:926-932 doi:10.16285/j.rsm.2017.1886
505 Ghobadi MH, Taleb Beydokhti AR, Nikudel MR, Asiabanha A, Karakus M (2016) The effect of freeze–thaw
506 process on the physical and mechanical properties of tuff Environmental Earth Sciences 75
507 doi:10.1007/s12665-016-5664-8
508 Hoek E, Brown ET (1997) Practical Estimates of Rock Mass Strength International Journal of Rock
509 Mechanics and Mining Sciences 34:1165-1186 doi:10.1016/S1365-1609(97)80069-X
510 Hoek E, Carranza-Torres C, Corkum B (2002) HOEK-BROWN FAILURE CRITERION – 2002 EDITION.
511 Paper presented at the Proc. NARMS-TAC Conference, Toronto,
512 Hosseini M, Khodayari AR (2019) Effect of freeze-thaw cycle on strength and rock strength parameters (A
513 Lushan sandstone case study) Journal of Mining and Environment 10:257-270
514 doi:10.22044/jme.2018.7619.1616
515 İnce İ, Fener M (2016) A prediction model for uniaxial compressive strength of deteriorated pyroclastic rocks
516 due to freeze–thaw cycle Journal of African Earth Sciences 120:134-140
517 doi:10.1016/j.jafrearsci.2016.05.001
518 Jamshidi A, Nikudel MR, Khamehchiyan M (2013) Predicting the long-term durability of building stones
519 against freeze–thaw using a decay function model Cold Regions Science and Technology 92:29-36
520 doi:10.1016/j.coldregions.2013.03.007
521 Jia H, Xiang W, Krautblatter M (2015) Quantifying Rock Fatigue and Decreasing Compressive and Tensile
522 Strength after Repeated Freeze-Thaw Cycles Permafrost and Periglacial Processes 26:368-377
523 doi:10.1002/ppp.1857
524 Kang K-S, Hu N-L, Sin C-S, Rim S-H, Han E-C, Kim C-N (2017) Determination of the mechanical
525 parameters of rock mass based on a GSI system and displacement back analysis Journal of Geophysics

526 and Engineering 14:939-948 doi:10.1088/1742-2140/aa6e78
527 Ke B, Zhou K, Xu C, Deng H, Li J, Bin F (2018) Dynamic Mechanical Property Deterioration Model of
528 Sandstone Caused by Freeze–Thaw Weathering Rock Mechanics and Rock Engineering 51:2791-2804
529 doi:10.1007/s00603-018-1495-0
530 Khanlari G, Sahamieh RZ, Abdilor Y (2014) The effect of freeze–thaw cycles on physical and mechanical
531 properties of Upper Red Formation sandstones, central part of Iran Arabian Journal of Geosciences
532 8:5991-6001 doi:10.1007/s12517-014-1653-y
533 Lai Y, Wu H, Wu Z, Liu S, Den X (2000) Analytical viscoelastic solution for frost force in cold-region
534 tunnels Cold Regions Science and Technology 31:227-234 doi:10.1016/S0165-232X(00)00017-3
535 Li J-l, Zhou K-p, Liu W-j, Deng H-w (2016) NMR research on deterioration characteristics of microscopic
536 structure of sandstones in freeze–thaw cycles Transactions of Nonferrous Metals Society of China
537 26:2997-3003 doi:10.1016/s1003-6326(16)64430-8
538 Li J, Kaunda RB, Zhou K (2018) Experimental investigations on the effects of ambient freeze-thaw cycling
539 on dynamic properties and rock pore structure deterioration of sandstone Cold Regions Science and
540 Technology 154:133-141 doi:10.1016/j.coldregions.2018.06.015
541 Li J, Zhou K, Zhang Y, Xu Y (2012) Experimental Study of Rock Porous Structure Damage Characteristics
542 Under Condition of Freezing-Thawing Cycles Based on Nuclear Magnetic Resonance Technique
543 Chinese Journal of Rock Mechanics and Engineering 31:1208-1214
544 Liu C, Deng H, Zhao H, Zhang J (2018) Effects of freeze-thaw treatment on the dynamic tensile strength of
545 granite using the Brazilian test Cold Regions Science and Technology 155:327-332
546 doi:10.1016/j.coldregions.2018.08.022
547 Liu C, Deng J, Yu S, Li P, Lin Y (2020) Effect of Freezing and Thawing on Microstructure Damage and
548 Dynamic Flexural Tension of Granite Rock Mechanics and Rock Engineering 53:3853-3858
549 doi:10.1007/s00603-020-02127-x
550 Liu Q, Huang S, Kang Y, Liu X (2015) A prediction model for uniaxial compressive strength of deteriorated
551 rocks due to freeze–thaw Cold Regions Science and Technology 120:96-107
552 doi:10.1016/j.coldregions.2015.09.013
553 Ma Q, Ma D, Yao Z (2018) Influence of freeze-thaw cycles on dynamic compressive strength and energy
554 distribution of soft rock specimen Cold Regions Science and Technology 153:10-17
555 doi:10.1016/j.coldregions.2018.04.014
556 Matsuoka N (2001) Direct observation of frost wedging in alpine bedrock Earth Surface Processes and
557 Landforms 26:601-614 doi:10.1002/esp.208
558 Matsuoka N (2008) Frost weathering and rockwall erosion in the southeastern Swiss Alps: Long-term (1994–
559 2006) observations Geomorphology 99:353-368 doi:10.1016/j.geomorph.2007.11.013

Momeni A, Abdilor Y, Khanlari GR, Heidari M, Sepahi AA (2016) The effect of freeze–thaw cycles on physical and mechanical properties of granitoid hard rocks Bulletin of Engineering Geology and the Environment:1649-1656 doi:10.1007/s10064-015-0787-9

Mutlutürk M, Altindag R, Türk G (2004) A decay function model for the integrity loss of rock when subjected to recurrent cycles of freezing–thawing and heating–cooling International Journal of Rock Mechanics and Mining Sciences 41:237-244 doi:10.1016/s1365-1609(03)00095-9

Nicholson DT, Nicholson FH (2000) Physical deterioration of sedimentary rocks subjected to experimental freeze-thaw weathering Earth Surf Process Landf Earth Surface Processes and Landforms 25:1295-1307 doi:10.1002/1096-9837(200011)25:12<1295::AID-ESP138>3.0.CO;2-E

Rummel F, Fairhurst C (1970) Determination of the post-failure behavior of brittle rock using a servo-controlled testing machine Rock Mechanics and Rock Engineering 2:189-204 doi:10.1007/BF01245574

Seyed Mousavi SZ, Tavakoli H, Moarefvand P, Rezaei M (2019) Assessing the effect of freezing-thawing cycles on the results of the triaxial compressive strength test for calc-schist rock International Journal of Rock Mechanics and Mining Sciences 123 doi:10.1016/j.ijrmms.2019.104090

Shen Y, Wang Y, Wei X, Jia H, Yan R (2020) Investigation on meso-debonding process of the sandstone–concrete interface induced by freeze–thaw cycles using NMR technology Construction and Building Materials 252 doi:10.1016/j.conbuildmat.2020.118962

Sun Y, Zhai C, Xu J, Cong Y, Qin L, Zhao C (2020) Characterisation and evolution of the full size range of pores and fractures in rocks under freeze-thaw conditions using nuclear magnetic resonance and three-dimensional X-ray microscopy Engineering Geology 271 doi:10.1016/j.enggeo.2020.105616

Tan X, Chen W, Yang J, Cao J (2011) Laboratory investigations on the mechanical properties degradation of granite under freeze–thaw cycles Cold Regions Science and Technology 68:130-138 doi:10.1016/j.coldregions.2011.05.007

Ulusay R (2015) The ISRM Suggested Methods for Rock Characterization, Testing and Monitoring 2007–2014. Springer International Publishing Switzerland. doi:10.1007/978-3-319-07713-0

Wang F, Cao P, Wang Y, Hao R, Meng J, Shang J (2020) Combined effects of cyclic load and temperature fluctuation on the mechanical behavior of porous sandstones Engineering Geology 266 doi:10.1016/j.enggeo.2019.105466

Wang L, Li N, Qi J, Tian Y, Xu S (2019) A study on the physical index change and triaxial compression test of intact hard rock subjected to freeze-thaw cycles Cold Regions Science and Technology 160:39-47 doi:10.1016/j.coldregions.2019.01.001

Wang P, Xu J, Liu S, Liu S, Wang H (2016a) A prediction model for the dynamic mechanical degradation of sedimentary rock after a long-term freeze-thaw weathering: Considering the strain-rate effect Cold

Regions Science and Technology 131:16-23 doi:10.1016/j.coldregions.2016.08.003

Wang P, Xu J, Liu S, Wang H (2016b) Dynamic mechanical properties and deterioration of red-sandstone subjected to repeated thermal shocks Engineering Geology 212:44-52 doi:10.1016/j.enggeo.2016.07.015

Wang P, Xu J, Liu S, Wang H, Liu S (2016c) Static and dynamic mechanical properties of sedimentary rock after freeze-thaw or thermal shock weathering Engineering Geology 210:148-157 doi:10.1016/j.enggeo.2016.06.017

Weng L, Wu Z, Taheri A, Liu Q, Lu H (2020) Deterioration of dynamic mechanical properties of granite due to freeze-thaw weathering_ Considering the effects of moisture conditions Cold Regions Science and Technology 176:1-15 doi:10.1016/j.coldregions.2020.103092

Yao M, Rong G, Zhou C, Peng J (2016) Effects of Thermal Damage and Confining Pressure on the Mechanical Properties of Coarse Marble Rock Mechanics and Rock Engineering 49:2043-2054 doi:10.1007/s00603-016-0916-1

Yavuz H (2010) Effect of freeze–thaw and thermal shock weathering on the physical and mechanical properties of an andesite stone Bulletin of Engineering Geology and the Environment 70:187-192 doi:10.1007/s10064-010-0302-2

Zhang F, Sheng Q, Zhu Z, Zhang Y (2008) Study on Post-Peak Mechanical Behaviour and Strain-Softening Model of Three Gorges Granite Chinese Journal of Rock Mechanics and Engineering 27:2651-2655

Zhang H et al. (2019a) A novel constitutive modelling approach measured under simulated freeze–thaw cycles for the rock failure Engineering with Computers doi:10.1007/s00366-019-00856-4

Zhang J, Deng H, Taheri A, Ke B, Liu C (2019b) Deterioration and strain energy development of sandstones under quasi-static and dynamic loading after freeze-thaw cycles Cold Regions Science and Technology 160:252-264 doi:10.1016/j.coldregions.2019.01.007

Zhang J, Fu H, Huang Z, Wu Y, Chen W, Shi Y (2019c) Experimental study on the tensile strength and failure characteristics of transversely isotropic rocks after freeze-thaw cycles Cold Regions Science and Technology 163:68-77 doi:10.1016/j.coldregions.2019.04.006

Zhang S, Lai Y, Zhang X, Pu Y, Yu W (2004) Study on the damage propagation of surrounding rock from a cold-region tunnel under freeze–thaw cycle condition Tunnelling and Underground Space Technology 19:295-302 doi:10.1016/j.tust.2003.11.011

Zhao J, Feng X-T, Zhang X-W, Zhang Y, Zhou Y-Y, Yang C-X (2018) Brittle-ductile transition and failure mechanism of Jinping marble under true triaxial compression Engineering Geology 232:160-170 doi:10.1016/j.enggeo.2017.11.008